ADVANCED MATERIALS
www.advmat.de

Hydroxyapatite Nanorods Function as Safe and Effective Growth Factors Regulating Neural Differentiation and Neuron Development

Min Hao, Zixian Zhang, Chao Liu, Yue Tian, Jiazhi Duan, Jianlong He, Zhaoyang Sun, He Xia, Shan Zhang, Shuhua Wang, Yuanhua Sang, Guogang Xing,* and Hong Liu**

Neural stem cell (NSC) transplantation is one of the most promising therapeutic strategies for neurodegenerative diseases. However, the slow spontaneous differentiation of NSCs often hampers their application in neural repair. Although some biological growth factors accelerate the differentiation of NSCs, their high cost, short half-life, and unpredictable behavior in vivo, as well as the complexity of the operation, hinder their clinical use. In this study, it is demonstrated that hydroxyapatite (HAp), the main component of bone, in the form of nanorods, can regulate the neural differentiation of NSCs and maturation of the newly differentiated cells. Culturing NSCs with HAp nanorods leads to the differentiation of NSCs into mature neurons that exhibit well-defined electrophysiological behavior within 5 days. The state of these neurons is much better than when culturing the cells without HAp nanorods, which undergo a 2-week differentiation process. Furthermore, RNA-sequencing data reveal that the neuroactive ligand–receptor interaction pathway is dominant in the enriched differentiated neuronal population. Hence, inorganic growth factors like HAp act as a feasible, effective, safe, and practical tool for regulating the differentiation of NSCs and can potentially be used in the treatment of neurodegenerative diseases.

1. Introduction

Neurodegenerative diseases (NDDs), such as brain injury, Alzheimer's disease, Parkinson's disease, and Huntington's disease, caused by the loss of neurons and/or myelin in the nervous system.[1] Some forms of treatment for NDDs that were based on the activation of resting neural stem cells (NSCs) displayed optimal therapeutic activity in animals but were found to be ineffective in humans. This difference has been attributed to the presence of endogenous NSCs throughout the rodent life cycle; however a similar observation has not been made in humans.[2] Allogeneic stem cell transplantation has provided a new route for the treatment of NDDs. In recent years, NSCs and induced pluripotent stem cells have frequently been used to treat NDDs because of their neural differentiation potential.[3] However, the spontaneous differentiation of NSCs and induced pluripotent stem cells is too slow and, hence, cannot be used directly for neural repair. Therefore, accelerated neural differentiation of NSCs into mature neurons is essential for the use of NSCs in the treatment of NDDs. Growth factors such as nerve growth factor (NGF), brain-derived neurotrophic factor, and vascular endothelial growth factor promote the differentiation of NSCs. However, this approach is limited due to their degradation in vivo and uncontrollable diffusion.[4]

In addition to biomolecules, calcium ions (Ca^{2+}) in the microenvironment play an important role in neurogenesis, particularly in regulating the proliferation, differentiation, and migration of NSCs.[5] Ca^{2+} is a powerful, highly ubiquitous, and versatile second messenger present in cells. Ca^{2+} signal

M. Hao, J. Duan, J. He, H. Xia, S. Zhang, Prof. S. Wang, Prof. Y. Sang, Prof. H. Liu
State Key Laboratory of Crystal Materials
Shandong University
Jinan 250100, P. R. China
E-mail: sangyh@sdu.edu.cn; hongliu@sdu.edu.cn

Z. Zhang, Y. Tian, Prof. G. Xing
Neuroscience Research Institute
Peking University
Beijing 100191, P. R. China
E-mail: ggxing@bjmu.edu.cn

The ORCID identification number(s) for the author(s) of this article can be found under https://doi.org/10.1002/adma.202100895.

DOI: 10.1002/adma.202100895

Dr. C. Liu, Z. Sun
Department of Oral and Maxillofacial Surgery
Qilu Hospital of Shandong University
Jinan 250012, P. R. China

Prof. S. Wang, Prof. Y. Sang
Advanced Medical Research Institute
Shandong University
Jinan 250100, P. R. China

Prof. H. Liu
Institute for Advanced Interdisciplinary Research (IAIR)
University of Jinan
Jinan 250022, P. R. China

transduction mainly occurs through the changes in cytoplasmic Ca^{2+} concentration after the opening of Ca^{2+} channels. Moreover, phosphorus plays an essential role in neurogenesis. Black phosphorus nanoscaffolds can induce angiogenesis and neurogenesis and accelerate calcium-dependent axon regrowth and remyelination.[6] The phosphates promote cellular attachment and axon extension, and phosphate-based nerve ducts are used to promote peripheral nerve regeneration.[7]

Equilibrium homeostasis in organisms is important in vivo. Any substantial instant release of ions causes dysfunction of the surrounding tissues.[8] Hence, controlled ion release to maintain homeostasis in vivo is required for drug designing. Recently, the regulation of stem cell fate using nanomaterials has been extensively studied.[9] The interaction between nanoparticles and stem cells begins with adherence of nanoparticles to the cellular membrane, followed by their subsequent entry into the cell through endocytosis or pores in the cell membrane.[10] The endocytosis of NSCs has been observed using inorganic nanomaterials of various sizes.[11] As a major component of teeth and bones, hydroxyapatite (HAp) is rich in calcium and phosphorus and exhibits excellent biocompatibility. Furthermore, HAp could promote the osteogenic differentiation of mesenchymal stem cells and human adipose-derived stem cells by building a calcium-rich microenvironment.[12] Hence, we postulated that HAp would affect the neural differentiation of NSCs by promoting the extracellular and intracellular release of Ca^{2+}, and the differentiation may be regulated when HAp nanorods are administered as a growth factor.

In this study, HAp nanorods, synthesized via a hydrothermal method, were added to NSCs culture, and their regulatory effects on the fate of NSCs were explored. Notably, HAp nanorods promoted neural differentiation and formation of mature neurons, as confirmed by assessing the gene and protein expression, and electrophysiological analyses of the newly differentiated neurons. Thus, HAp nanorods with slow-release and long-lasting properties may potentially be used in the treatment of NDDs.

2. Results and Discussion

2.1. HAp Nanorods Possess Good Cytocompatibility in Mouse NSCs (mNSCs)

The HAp nanorods (length, 80–100 nm; width, 30–50 nm) were synthesized using the hydrothermal method and exhibited a highly uniform morphology (**Figure 1**a). Using high-resolution transmission electron microscopy (HRTEM), we observed that an individual nanorod exhibited an interplanar crystal spacing of 0.28 nm, corresponding to the 300 planes of the hexagonally structured $Ca_{10}(PO_4)_6(OH)_2$, along with good crystallinity of HAp (Figure 1b).[13] Moreover, the X-ray diffraction (XRD) pattern (Figure 1c) confirmed that all the peaks were assigned to the HAp structure (ICSD card no. 74-0566).[14] A homogenous HAp nanorod suspension was prepared for use in the biological experiments.

For evaluating the neural differentiation of Mouse NSCs, the quality and viability of the isolated mNSCs were assessed. Nestin, a filamentous protein, is typically expressed in NSCs and is associated with the stemness of the cells; hence, nestin is regarded as a neuronal stem/progenitor cell marker.[15] Immunostaining for assessment of nestin expression revealed the immense multi-differentiation potential of the isolated mNSCs (Figure S1, Supporting Information). The live/dead cell staining and cell counting kit-8 (CCK-8) were used to qualitatively and quantitatively evaluate the cytocompatibility of HAp nanorods with mNSCs. After culturing with different concentrations of HAp nanorods for 48 h, live/dead cellular staining was conducted (Figure 1d). The live cells were stained with calcein AM, while dead cells were stained with propidium iodide (PI). Numerous live cells and only a few dead cells were observed, based on the normal apoptosis rate. The percentage of surviving mNSCs that were cultured with different concentrations of HAp nanorods was determined (Figure S2, Supporting Information). The percentage of surviving mNSCs cultured with or without HAp nanorods was greater than 95% (Figure 1e), and no notable difference in the survival rate was observed among the samples treated with or without HAp nanorods, thus confirming the good cytocompatibility of HAp nanorods. The effect of different concentrations of HAp nanorods on the proliferation of mNSCs after 1, 2, and 3 days of culture was evaluated using the CCK-8 assay (Figure 1f). Notably, the dehydrogenase activity in mNSCs cultured with 150 μg mL^{-1} and 200 μg mL^{-1} HAp nanorods increased on day 3 compared with the other groups. However, cells cultured with increased concentrations (300 and 400 μg mL^{-1}) of HAp nanorods showed dehydrogenase activity similar to that of the control. Thus, stimulation of mNSCs with an appropriate amount of HAp nanorods promoted cell proliferation, while exposure to an excess of HAp nanorods countered this effect. A high concentration of HAp nanorods can possibly promote cell differentiation, as a decrease in proliferation has been reported prior to differentiation.[16] While a small change was observed in the first two days for all samples, the effect of HAp on mNSC fate became significant after the third day.

Additionally, immunostaining for F-actin and nestin was performed to determine the spread and the stemness of mNSCs, respectively (Figure 1g). All samples cultured with varying concentrations of HAp nanorods expressed the NSC marker nestin, confirming the stemness of the cells. Figure 1h summarized the expected role of HAp in mNSC differentiation, more mature neurons were produced when mNSCs were cultured with HAp nanorods. HAp nanomaterials with other morphologies were also studied for mNSC differentiation. However, HAp nanorods exhibited a better effect on mNSC differentiation than HAp spheres and HAp nanowires (Figures S3 and S4, Supporting Information). Hence, HAp nanorods were used to explore the role of HAp in mNSC differentiation.

2.2. HAp Nanorods Regulate the mRNA and Protein Expression in mNSCs

Next, the mNSCs were cultured in neurobasal differentiation medium supplemented with 0, 100, 150, 200, 300, or 400 μg mL^{-1} HAp nanorods for 7 days. The expression of neural-specific markers, including nestin, βIII tubulin (Tuj1), glial fibrillary acid protein (GFAP), microtubule-associated protein 2 (MAP2),

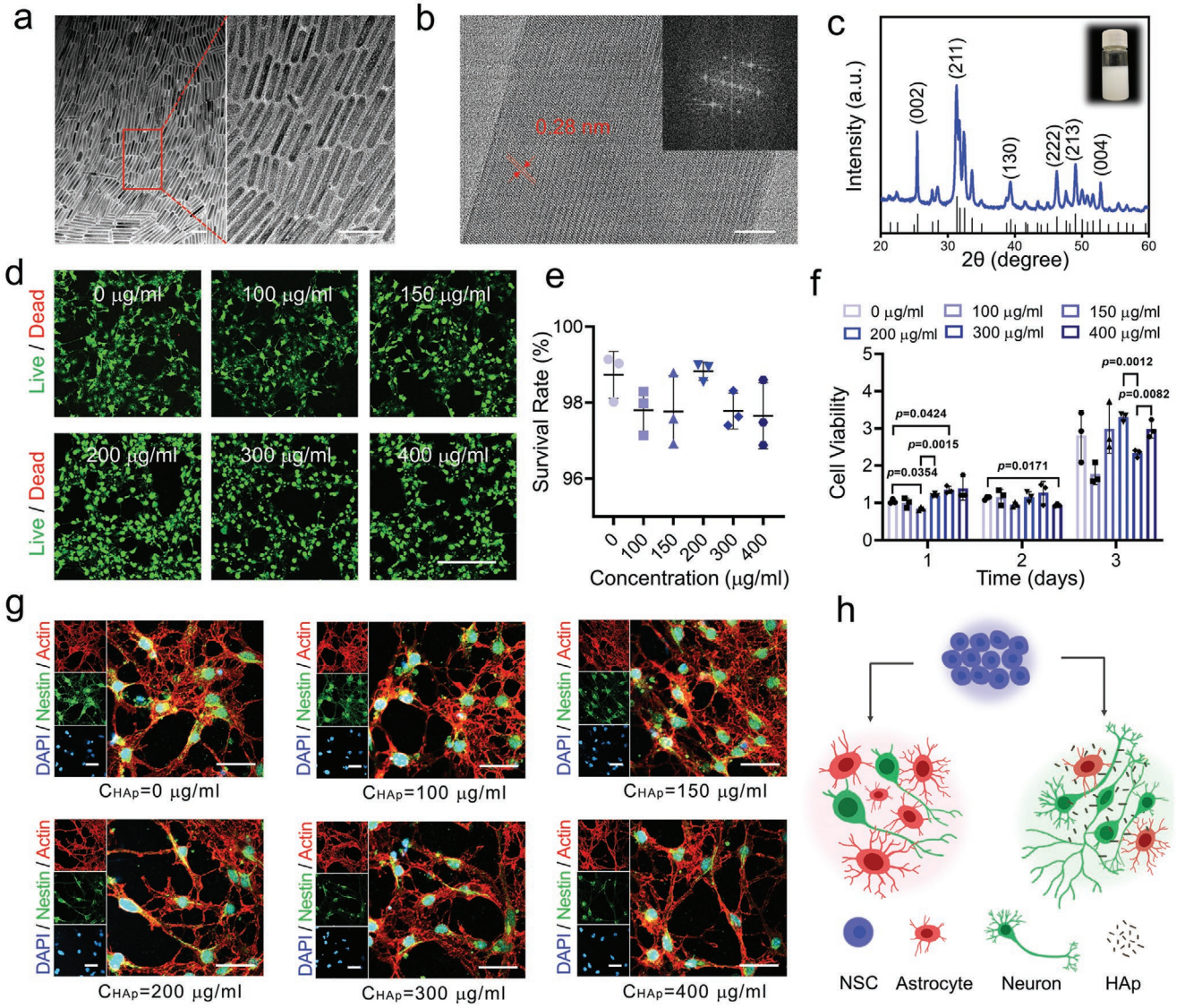

Figure 1. Characterization and cytocompatibility of HAp nanorods. a) TEM image of HAp nanorods. Scale bars: 50 nm. b) HRTEM image of HAp nanorods. Scale bar: 5 nm. The inset shows the fast Fourier transform image. c) XRD pattern of HAp nanorods. Inset shows the HAp nanorod suspension used in the experiments. d) Representative live/dead staining images of the mNSCs after culturing with different concentrations of HAp nanorods for 48 h. The live cells are stained green, and the dead cells are stained red. Scale bar: 200 μm e) Percentage of surviving mNSCs after culturing with different concentrations HAp nanorods for 48 h. At least 500 cells from three randomly selected fields were counted to calculate the survival rate. f) Analysis of proliferating mNSCs cultured with different concentrations of HAp nanorods normalized to control conditions on day 1. Data are presented as mean ± standard deviation (SD). The *p* values were calculated using two-way analysis of variance (ANOVA) with Bonferroni's comparison test. g) Immunostaining for F-actin, nestin, and nuclei for 48 h. F-actin is shown in red, nestin is shown in green, and nuclei are stained blue. Scale bars: 30 μm. h) Schematic depicting the expected role of HAp in mNSC differentiation.

and neurogenic differentiation 1 (Neurod1), were determined using real-time quantitative polymerase chain reaction (RT-qPCR) after 7 days (**Figure 2**a). RT-qPCR analysis was performed by normalizing the relative mRNA expression level of the target genes to that of the control (0 μg mL^{-1}). When NSCs were cultured in neurobasal differentiation medium supplemented with HAp nanorods, the relative expression of nestin mRNA declined slightly, indicating that the administration of HAp nanorods to NSCs reduced the stemness of NSCs and may promote neural differentiation. Tuj1 is a specific marker of early neurons, that is crucial for neurite outgrowth. Therefore, the upregulation and post-translational processing of Tuj1 are believed to be essential during neuronal differentiation.[17] As the concentration of HAp nanorods increased from 100 to 150, 200, 300, and 400 μg mL^{-1}, Tuj1 mRNA expression increased by 4.5-, 7.0-, 8.2-, 7.7-, and 12.4-fold compared with the control, respectively. High Tuj1 expression levels confirmed the induction of neuronal differentiation in mNSCs. GFAP is mainly distributed in astrocytes of the central nervous system and is involved in the construction of the cytoskeleton and maintenance of its tensile strength.[18] The relative expression of GFAP mRNA in mNSCs cultured with HAp nanorods

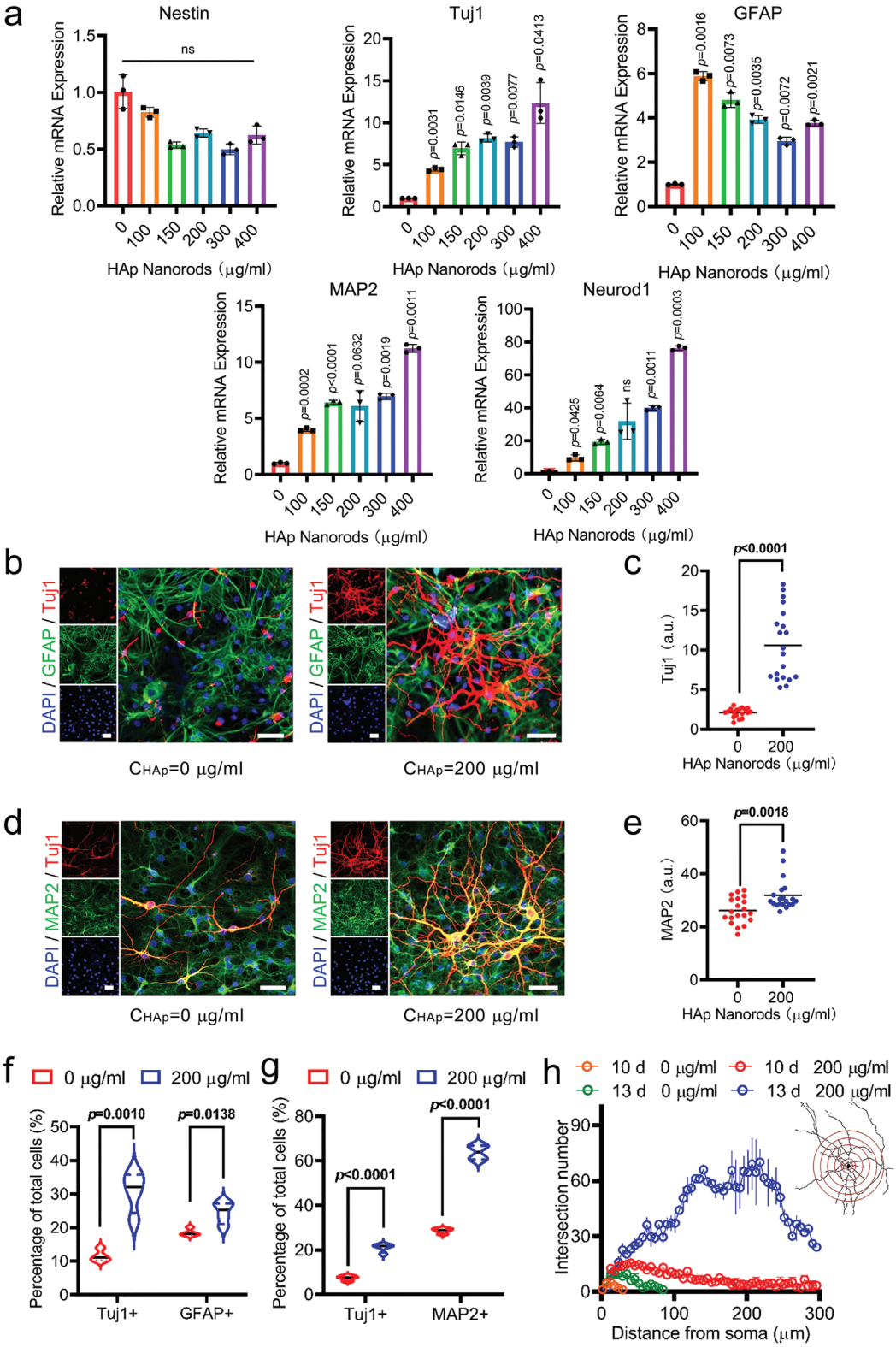

Figure 2. Analysis of mRNA and protein expression. a) RT-qPCR analysis of the expression of the neuron-specific genes nestin, Tuj1, GFAP, MAP2, and Neurod1 in mNSCs cultured with different concentrations HAp nanorods for 7 days. Data are presented as mean ± SD. The *p* values were calculated using one-way ANOVA with Bonferroni's comparison test. ns: not significant. b,c) Representative immunostaining images for the neural-specific markers Tuj1, GFAP, and nuclei, and statistical analysis of the mean Tuj1 fluorescence intensity in mNSCs cultured with 0 and 200 μg mL^{-1} HAp nanorods for 10 days. d,e) Tuj1, MAP2, and nucleus staining, and the statistical analysis of the mean MAP2 fluorescence intensity in the mNSCs after 13 days of culture with 0 and 200 μg mL^{-1} HAp nanorods. Cell nuclei were stained blue with 4′,6-diamidino-2-phenylindole (DAPI), Tuj1 is shown in

at concentrations of 100, 150, 200, 300, and 400 μg mL^{-1} were 5.9-, 4.8-, 3.9-, 3.0-, and 3.8-fold higher than that in the control cells, respectively. Thus, HAp nanorods exerted a positive effect on GFAP expression. However, a decreasing trend in GFAP expression was observed with increasing HAp concentration, inverse of the increasing trend of Tuj1 expression. This finding implied that HAp had a greater effect on Tuj1 expression than GFAP expression. MAP2 is mainly present in the cell body, dendrites, and dendritic spines of neurons in normal brain tissue. Additionally, MAP2 is one of the most abundant proteins in the brain and is involved in processes such as protuberance growth, cytoplasmic protein transport, and neuronal shape determination. The developmental regulation of Tuj1 and MAP2 expression contributes to the unique stability of neuronal microtubules.[17b,19] MAP2 expression levels in cells treated with 100, 150, 200, 300, and 400 μg mL^{-1} HAp nanorods were 4.0-, 6.4-, 6.1-, 7.0-, and 11.2-fold higher than that in the control, respectively. The trend of MAP2 expression was similar to that of Tuj1 expression and was consistent with the tight relationship between MAP2 and Tuj1 during neural development. As MAP2 is a marker of mature neurons, the increase in MAP2 expression observed in mNSCs treated with HAp nanorods indicates that HAp nanorods exert a neural repair-promoting effect. Neurod1, a pro-neural basic helix–loop–helix transcription factor, is prominently expressed late in the development of the nervous system and is therefore more likely to be involved in the survival, terminal differentiation, and neuronal maturation.[20] Neurod1 expression levels were increased 9.6-fold (100 μg mL^{-1}), 19.5-fold (150 μg mL^{-1}), 31.9-fold (200 μg mL^{-1}), 40.0-fold (300 μg mL^{-1}), and 76.5-fold (400 μg mL^{-1}). Neurod1 expression showed a trend similar to that of Tuj1 and MAP2 expression. Additionally, the high expression level indicated a high possibility of nerve function after 7 days of culture. In summation, the expression of the stemness gene nestin decreased, while the expression of the neural differentiation genes Tuj1 and GFAP increased after mNSCs were cultured with different concentrations of HAp nanorods for 7 days. Therefore, it can be concluded that HAp nanorods accelerate NSC differentiation and may promote neuronal maturation, based on the high levels of MAP2 and Neurod1 expression. Furthermore, HAp nanorods administered at a concentration of 200 μg mL^{-1} have been reported to enhance the osteogenic differentiation of bone marrow-derived mesenchymal stem cells in vitro and can be regarded as an optimal choice for targeting stem cells.[11] Indeed, combined with the results of the CCK-8 assay, HAp nanorods at the concentration of 200 μg mL^{-1} showed a balanced property in regulating cell activity and comprehensive cell differentiation; hence, this concentration was used in all the subsequent experiments.

Immunostaining was carried out for assessing the number of nuclei, Tuj1, and GFAP expression in mNSCs cultured for 10 days (Figure 2b). The number of nuclei in cells cultured with 0 and 200 μg mL^{-1} of HAp nanorods was similar, consistent with the prior results of cell viability after culture with and without HAp nanorods (Figure 1). However, a greater number of cells cultured with HAp nanorods express Tuj1 than cells cultured without HAp nanorods. Additionally, mNSCs cultured with HAp nanorods showed an increased number of axons, tighter intercellular connections, and an obvious morphology of neurons (Figure S5, Supporting Information). The cells expressing GFAP also showed differences, but the differences were not significant. Figure 2c shows the mean Tuj1 fluorescence intensity from 20 images of randomly selected fields of mNSCs after 10 days of culture. Tuj1 expression in HAp-stimulated mNSCs was ≈5.0-fold higher than that in the control. As MAP2 is a marker of mature neurons and is expressed at high levels during mNSC neuronal differentiation, immunostaining of the nuclei, Tuj1 and MAP2 were also performed in mNSCs cultured for 13 days (Figure 2d). Similar to mNSCs cultured for 10 days, the number of nuclei in cells cultured with 0 and 200 μg mL^{-1} HAp nanorods was similar, showing a comparable cell density. A greater number of cells cultured with HAp nanorods expressed Tuj1 than cells cultured without HAp nanorods. The number of cells expressing MAP2 also differed. The mean MAP2 fluorescence intensity was quantified from 20 images of randomly selected fields of view of mNSCs after 13 days of culture (Figure 2e). MAP2 expression in HAp-treated mNSCs was ≈1.3-fold higher than that in the control. The percentages of Tuj1$^+$ and GFAP$^+$ cells in the cell populations treated with 0 and 200 μg mL^{-1} HAp nanorods for 10 days were calculated and normalized to nuclei (Figure 2f).[17b,21] A detailed description of the analysis process has been provided (Figure S6, Supporting Information). Interestingly, the mNSCs cultured without HAp nanorods differentiated into Tuj1$^+$ neurons (average ratio, 12.0%) and GFAP$^+$ astrocytes (average ratio, 18.8%), indicating that mNSCs were more likely to spontaneously differentiate into astrocytes. On the contrary, cells treated with HAp nanorods differentiated into Tuj1$^+$ neurons (average ratio, 33.6%) and GFAP$^+$ astrocytes (average ratio, 25.9%). The proportion of early neurons increased to 21.6% and the proportion of astrocytes only increased to 7.1% after mNSCs were cultured with HAp nanorods. Based on these findings, the administration of HAp nanorods increased the generation of neurons and regulated the direction of cell differentiation. In addition, the percentages of Tuj1$^+$ cells and MAP2$^+$ cells in the cell populations treated with 0 and 200 μg mL^{-1} HAp nanorods for 13 days were calculated and normalized to nuclei (Figure 2g). In mNSCs cultured without HAp nanorods, the average percentage of Tuj1$^+$ early neurons was 7.4%, and the average percentage of MAP2$^+$ mature neurons was 28.6%. The addition of HAp nanorods increased the percentage of Tuj1$^+$ early neurons to 21.0% and the percentage of MAP2$^+$ mature neurons to 63.8%. Only a 13.6% increase in the percentage of early neurons and a 35.2% increase in the percentage of mature

red, while GFAP or MAP2 is shown in green. Scale bars in (b) and (d): 30 μm. f,g) The percentage of Tuj1$^+$, GFAP$^+$, or MAP2$^+$ cells was calculated and normalized to nuclei in the cell populations treated with 0 and 200 μg mL^{-1} HAp nanorods for 10 days (f) and 13 days (g). At least 500 DAPI$^+$ cells were counted from each group. c,e,f,g) Data were analyzed using two-tailed unpaired Student's *t*-test. h) Sholl analysis of the dendritic complexity of neurons after mNSCs were cultured with 0 and 200 μg mL^{-1} HAp nanorods for 10 and 13 days. The Sholl analysis was performed on at least five neurons from each group.

neurons were observed. Neuronal maturation was observed in these groups (with HAp nanorods). Thus, in the late stage of culture, HAp nanorods mainly accelerate the maturation of neurons. Furthermore, GFAP expression was assessed in the cell populations treated with 0 and 200 μg mL^{-1} HAp nanorods for 13 days. Similar levels of GFAP expression were observed in cells cultured for 10 and 13 days, providing further support for the observation of increased expression of Tuj1 (Figure S7, Supporting Information). Based on the results of the concentric circle (Sholl) analysis, the complexity and maturation of neurons were increased in mNSCs cultured with 200 μg mL^{-1} HAp nanorods compared with mNSCs cultured without HAp nanorods for 10 days; a similar trend was observed at 13 days. The maximum number of intersections was far less than 30 in mNSCs cultured without HAp for 13 days. At a distance of 300 μm from the soma, neurons were observed, and the maximum number of intersections exceeded 60 in mNSCs cultured with HAp for 13 days (Figure 2h and Figure S8, Supporting Information), indicating that the administration of HAp nanorods plays an important role in regulating the complexity and maturation of neurons.

2.3. HAp Nanorods Promote the Maturation of Neurons

Next, we performed an in-depth analysis of mNSCs cultured with 0 and 200 μg mL^{-1} HAp nanorods (**Figure 3**). First, we assessed the expression of nestin, Tuj1, MAP2, and GFAP mRNAs at different time points (0, 1, 3, 5, 7, and 10 days) in mNSCs cultured with 0 and 200 μg mL^{-1} HAp nanorods to compare the extent to which HAp nanorods accelerated neuronal maturation (Figure 3a). The relative expression of nestin mRNA decreased gradually when NSCs were cultured with HAp nanorods, and their expression was lower than that in cells cultured without HAp nanorods at the corresponding time points. The expression of Tuj1 indicated that more early neurons were produced from mNSCs cultured with HAp nanorods for 3 days than in mNSCs cultured without HAp nanorods for

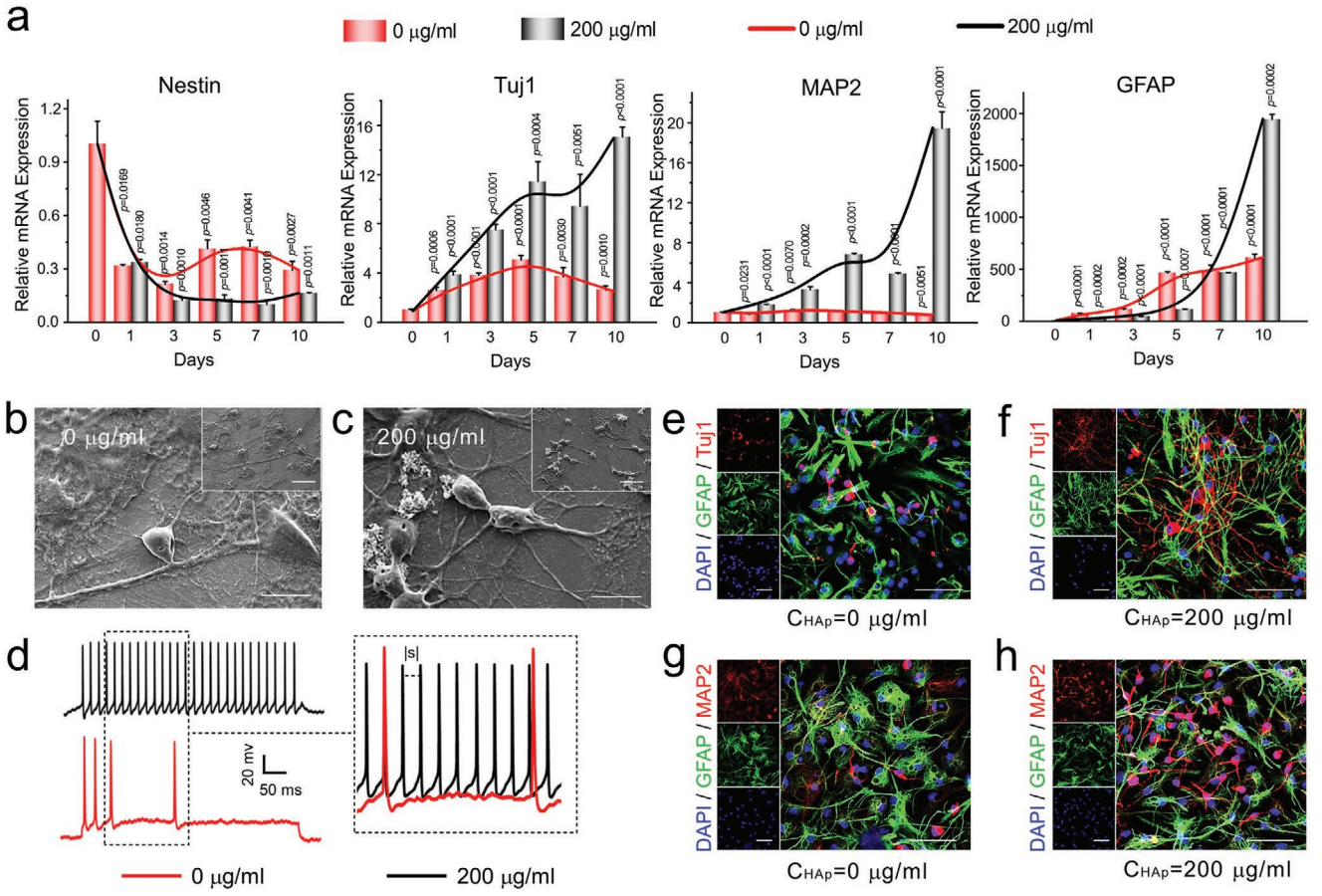

Figure 3. A detailed analysis of the characteristics of mNSCs cultured with 0 and 200 μg mL^{-1} HAp nanorods. a) RT-qPCR analysis to assess the expression of the neuron-specific genes nestin, Tuj1, MAP2, and GFAP in mNSCs cultured with different concentrations of HAp nanorods at different time points. Data are presented as mean ± SD. The *p* values were calculated using two-tailed unpaired Student's *t*-test. b,c) Scanning electron microscopy (SEM) images of mNSCs cultured with 0 (b) and 200 μg mL^{-1} (c) HAp nanorods. Scale bars: 8 μm (the scale bars of the inset is 20 μm). d) Electrophysiological analysis of NSCs cultured with 0 and 200 μg mL^{-1} HAp nanorods for 5 days. e,f) Representative images of immunostaining for the neural-specific markers Tuj1 and GFAP, and nuclear staining of mNSCs cultured with 0 (e) and 200 μg mL^{-1} (f) HAp nanorods for 5 days. g,h) MAP2, GFAP, and nuclear staining in the mNSCs after 5 days of culture with 0 (g) and 200 μg mL^{-1} (h) HAp nanorods. Cell nuclei are stained blue with DAPI, Tuj1 and MAP2 are shown in red, and GFAP is shown in green. e–h) Scale bars: 50 μm.

3 days, and similar results were obtained at 5, 7, and 10 days. A similar trend was observed for MAP2 expression. During the early stage of differentiation, GFAP was expressed at lower levels in HAp-treated mNSCs than in mNSCs cultured without HAp for 1, 3, and 5 days. After 10 days, more astrocytes and neurons were produced from HAp-treated mNSCs than from mNSCs cultured without HAp. Indeed, astrocytes can establish numerous small contacts with neurons and exhibit neuroprotective functions. Additionally, high GFAP expression promotes restoration of neural function. In order to explore the functional maturation of neurons generated after the neuronal differentiation of mNSCs induced by HAp nanorods, the cellular morphology and electrophysiology were analyzed, and immunostaining was performed on mNSCs cultured with HAp nanorods (0 and 200 μg mL^{-1}) for 5 days (Figure 3b–h). The morphology of mNSCs cultured with 0 and 200 μg mL^{-1} HAp nanorods is presented in Figure 3b,c, respectively. When the cells were cultured with HAp nanorods, more neuronal somas were detected. Electrophysiological analysis was performed with cultured mNSCs (Figure 3d and Figure S9, Supporting Information). Moreover, electrophysiological analysis of cultured mNSCs was performed using current clamp recordings to analyze the voltage difference across the cellular membrane.[17b,22] After culturing with HAp nanorods, the cells produced more action potentials (AP) with regular pulses over a long period, with a frequency of ≈25 Hz. The cells cultured without HAp nanorods showed irregular spikes, indicating that they were neuronal cells with electrophysiological activity but were not mature neurons. Based on these results, the neurons derived from the neural differentiation of mNSCs can be regulated by HAp nanorods, and these neurons mature and become functional earlier than cells cultured without HAp nanorods. In order to support these results further, immunostaining for Tuj1, GFAP, and MAP2 was performed in the cultured mNSCs. Tuj1, GFAP, and MAP2 were all expressed at higher levels in the mNSCs cultured with HAp nanorods (Figure 3f,h) than in cells cultured without HAp nanorods (Figure 3e,g), indicating that more neurons and astrocytes were generated from neural differentiation of mNSCs treated with HAp nanorods. Balanced neural differentiation into neurons and astrocytes promotes neuronal maturation. The data presented in Figure 3 are consistent with this result, although the cells were only cultured for 5 days. Thus, based on the comprehensive analyses of cell morphology, function, and protein expression, we propose that HAp nanorods resulted in the production of mature, functional neurons and astrocytes.

2.4. Localization of HAp Nanorods in the mNSCs and Lysosomes

The interaction between the HAp nanorods and mNSCs needs to be elucidated in order to discuss the mechanism by which HAp nanorods regulate the fate of mNSCs. TEM was performed on mNSCs cultured for 10 h with and without HAp nanorods (**Figure 4**a,b). Some HAp nanorods were detected in the cell (Figure 4b), confirming that the cells endocytosed the nanorods. Other HAp nanorods were located near the cell (inset of Figure 4b) and adhered to the cell membrane. The concentration of HAp nanorods applied to the cells exceeded the endocytosis capability of the mNSCs, ensuring a sufficient supply of HAp nanorods for each cell. Using the fluorescence properties of terbium:HAp (Tb:HAp) and LysoTracker (Figures S10 and S11, Supporting Information), the endocytosis of mNSCs was studied using a confocal laser scanning microscope (CLSM; Figure 4c and Figure S11, Supporting Information). After culturing mNSCs with 200 μg mL^{-1} Tb:HAp nanorods for 10 h, the fluorescent areas coincided with the location of mNSCs in the bright-field image and image of lysosomes. Therefore, the Tb:HAp nanorods are engulfed by lysosomes in cells or adhere to the surface of cell membranes. It is unclear whether endocytosis is required for HAp to exert the described effects. Figure 4d illustrates the relationship between the locations of the cell and HAp nanorods, such as adhered to the cell membranes, engulfed by the cell, or present in lysosomes.

2.5. Mechanism of Enhanced mNSC Neurogenesis by HAp Nanorods

In order to further elucidate the molecular mechanism by which HAp nanorods promoted the neural differentiation of mNSCs, RNA sequencing was performed using mNSCs cultured with 0 and 200 μg mL^{-1} HAp nanorods for 24 h. The differentially expressed genes in the mNSCs cultured with and without HAp nanorods are presented in the heat map, showing the upregulated expression of 52 genes and downregulated expression of 161 genes (Figure S12, Supporting Information). **Figure 5**a illustrates the most significantly differentially regulated genes, including 50 upregulated and 50 downregulated genes. Briefly, many of the upregulated genes were involved in neural differentiation and development of the nervous system, while many of the downregulated genes were involved in cell proliferation. For instance, among the upregulated genes, ETS variant transcription factor 4 (Etv4) and transcription factor 5 (Etv5) are members of the Pea3 family that are expressed in hippocampal neurons during the main period of dendritic development. They are also important physiological regulators of dendritic growth in the developing hippocampus.[23] NGF is a mature functional neurotrophic factor that regulates the structure and plasticity of neurons in the central nervous system.[24] ATPase-type 13A4 (ATP13A4) is a P5 subfamily transporter that facilitates cation transport across biological membranes. ATP13A4 expression increases during neurogenesis and plays an important role in early neuronal development.[25] Notably, ATP13A4 may be involved in regulating calcium signaling, which may promote the interaction between HAp nanorods and mNSCs. Among the downregulated genes, tumor necrosis factor receptor-associated factor 1 (TRAF1) plays an important role in neuroprotection, as an increase in TRAF1 expression results in increased neuronal death and the expansion of ischemic injury, while the lack of TRAF1 is neuroprotective.[26] Claudin 9 (Cldn 9) belongs to the claudin family of integral membrane proteins that are components of tight junctions. Cldn 9 is a tight junction protein that is expressed during the growth and development of the kidney and is involved in developmental regulation.[27] From the upregulated genes, 14 genes were randomly selected and analyzed using RT-qPCR (Figure 5b). All 14

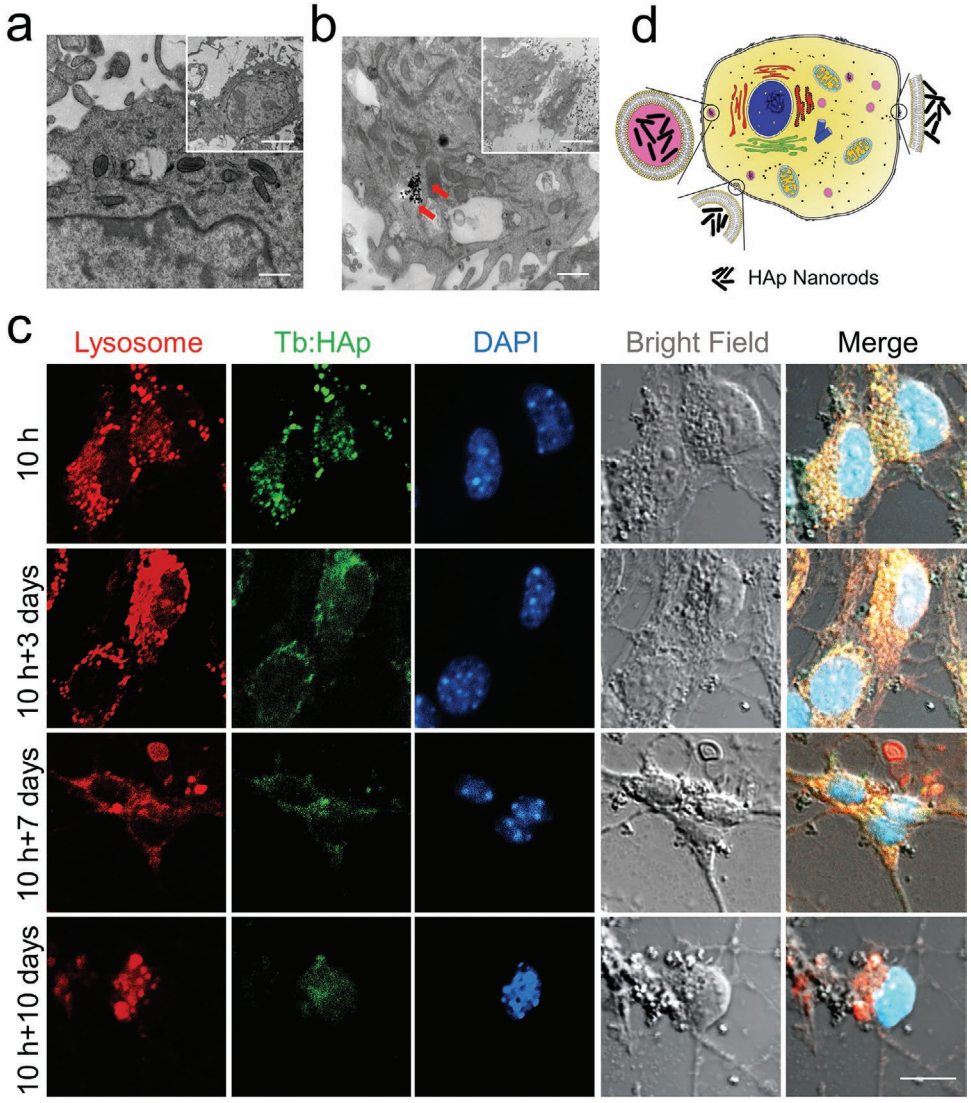

Figure 4. TEM and CLSM images of mNSCs cultured with Tb:HAp nanorods (concentration = 200 μg mL^{-1}). a,b) TEM images of mNSCs cultured with 0 (a) and 200 μg mL^{-1} (b) HAp nanorods for 10 h. Scale bars: 1 μm (the scale bar of the inset is 5 μm). c) Representative fluorescence images of lysosomes, Tb:HAp, and nuclei; bright-field images, and merged images of mNSCs cultured with Tb:HAp nanorods (green; concentration = 200 μg mL^{-1}) for 10 h, 10 h + 3 days, 10 h + 7 days, and 10 h + 10 days are shown. Lysosomes were stained with LysoTracker (red), and nuclei were stained with DAPI (blue). Scale bar: 20 μm. d) Schematic displaying the relationship between the locations of the NSC and HAp nanorods.

genes were upregulated in cells stimulated with HAp nanorods, consistent with the RNA-sequencing data. In order to further reveal the mechanism involved in HAp nanorod-enhanced mNSC neurogenesis, including specific molecular pathways and cellular events, we carried out differential gene–gene interaction network analysis (Figure 5c). Most of the differentially expressed genes can form their own networks and connections. Next, the related differentially regulated genes were analyzed using the Kyoto Encyclopedia of Genes and Genomes (KEGG) enrichment analysis to identify the top 30 pathways that were enriched in mNSCs cultured with and without HAp nanorods for 24 h (Figure 5d). Among these pathways, the neuroactive ligand–receptor interaction pathway belongs to neuron-enriched pathways, and the G protein-coupled receptor 83 (Gpr83), 5-hydroxytryptamine receptor 6 (Htr6), and glutamate receptor metabotropic 3 (Grm3) were involved in the neuroactive ligand–receptor interaction pathway. All these pathways were significantly upregulated after the initiation of neural differentiation (Figure 5a).[28] Furthermore, gene ontology (GO) analysis indicated that the upregulated genes were associated with postsynaptic density, excitatory synapse, inorganic cation transmembrane transporter activity, and central nervous system development, while the downregulated genes were associated with the proteinaceous extracellular matrix, growth, and regulation of cell proliferation (Figure 5e). Combined with the top 30 GO enrichments (Figure S13, Supporting Information), the cellular behavior was primarily associated with integrin binding, extracellular matrix binding, and Ca^{2+} regulation. Many pathways were involved in neurogenesis based on the KEGG analysis (Figure S14, Supporting Information). Thus, we

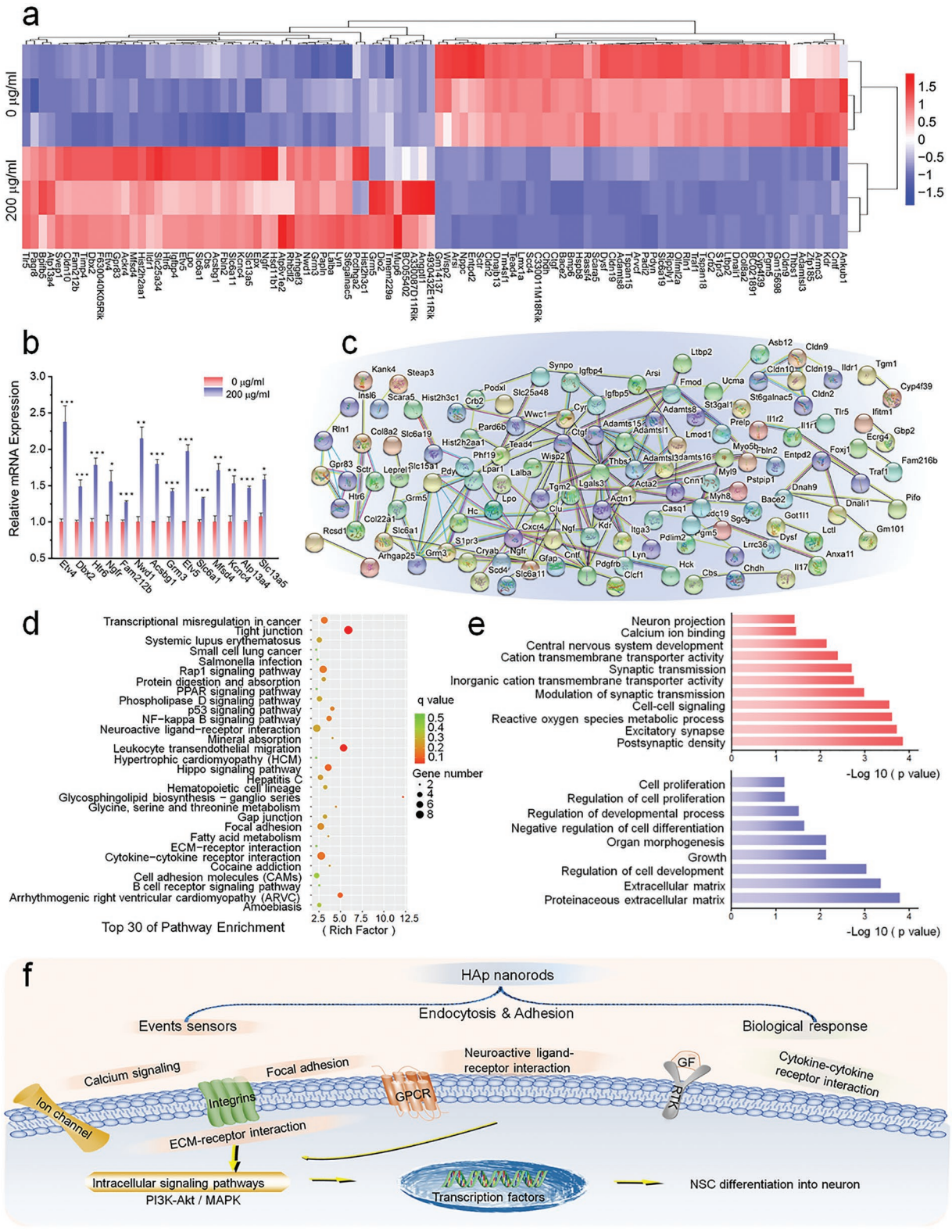

Figure 5. Mechanism underlying mNSC differentiation based on RNA sequencing. a) Heat map showing the differentially expressed genes between mNSCs cultured with 0 and 200 μg mL^{-1} HAp nanorods. b) RT-qPCR analysis of the expression of some upregulated genes shown in (a). Data are presented as mean ± SD. The *p* values were calculated using a Student's *t*-test. c) Differential gene–gene interaction networks for mNSCs cultured with 0 and 200 μg mL^{-1} HAp nanorods. d) Top 30 enriched pathways identified in mNSCs cultured with 0 and 200 μg mL^{-1} HAp nanorods for 24 h. e) GO analysis of the functional annotations of differentially expressed genes, including upregulated genes (top) and downregulated genes (bottom). f) Schematic illustration of enhanced mNSC neurogenesis by HAp nanorods.

propose that a possible mechanism of enhanced mNSC neurogenesis is promoted by the administration of HAp nanorods in the mNSC culture (Figure 5f). Based on our results, we predict that the interactions include endocytosis and adhesion of HAp nanorods to the cell membrane. When the HAp nanorods attach to the cell membrane, the focal adhesion signaling pathways are activated, and the associated ECM–receptor interaction and cytokine–cytokine receptor interaction form the key bridge of signal transduction and feedback between the HAp nanorods and cells.[29] Once the HAp nanorods are endocytosed, the released Ca^{2+} from lysosome activates the calcium signaling pathway. A 13.0-fold upregulation Gpr83 in mNSCs induced by HAp nanorods indicated the activation of the neuroactive ligand–receptor interaction pathway that influences the intracellular and extracellular signaling pathways.[30] The neuroactive ligand–receptor interaction can also activate the MAPK and PI3K–Akt signaling pathways, thereby regulating neuronal differentiation.[30] Thus, HAp nanorods can be regarded as a growth factor for regulating the neural differentiation of mNSCs, contributing substantially to the generation of neurons.

2.6. HAp Nanorods Induce Neuron Generation In Vivo

In order to further analyze the survival and differentiation of mNSCs in vivo after 5, 10, and 13 days (**Figure 6**a and Figure S15, Supporting Information), the mNSCs that had been cultured with 0 and 200 μg mL^{-1} HAp nanorods were encapsulated in Matrigel and subcutaneously injected into the backs of C57/BL6 mice toward the extremities. As expected, hematoxylin and eosin (H&E) staining showed no inflammation at the interface of the HAp nanorod-treated mNSCs embedded in Matrigel and the tissue after 5, 10, and 13 days (Figure 6b). Over time, more cells with neuronal morphology appeared (inset in Figure 6b). Immunostaining of tissue slices for the neuron-specific markers Tuj1 and MAP2 (Figure 6c) demonstrated that more neurons were produced from mNSCs cultured with HAp nanorods than from cells cultured without HAp nanorods for the corresponding number of days. Thus, HAp nanorods displayed a high potential for nerve repair, based on the positive regulatory effect on mNSCs.

3. Conclusion

We have assessed the potential of an inorganic nanomaterial, HAp nanorod, to promote the differentiation and maturation of NSCs by functioning. The regulatory effect of HAp nanorods on the fate of NSCs was confirmed by analyzing the expression of neural-specific genes and proteins. Additionally, electrophysiological analysis revealed AP from mature neurons, suggesting that HAp nanorods promoted the differentiation of mNSCs into mature and functional neurons. Many genes related to neural differentiation and the development of the nervous system were upregulated in cells cultured with HAp nanorods, while genes involved in cell proliferation were downregulated. Finally, we also demonstrated that the administration of HAp nanorods to mNSCs promoted the survival of mNSCs and neuronal differentiation in vivo. Thus, the strong effect of HAp nanorods on NSC differentiation and maturation indicates that HAp is an ideal candidate for slow-release and long-acting treatment for nerve repair.

4. Experimental Section

Chemicals and Reagents: For material synthesis, none of the chemicals and reagents were further purified. $Ca(NO_3)_2{\cdot}4H_2O$ (99.0%), oleic acid, $Na_3PO_4{\cdot}12H_2O$ (98%), and absolute ethanol (99.7%) were purchased from Sinopharm (Shanghai, China), whereas 1-octadecylamine (98%), cyclohexane (99.5%), and $Tb(NO_3)_3{\cdot}5H_2O$ (99.9%) were purchased from Aladdin (China).

For the mNSC experiments, neurobasal medium, glutaMAX-1, fetal bovine serum (FBS), B-27 supplement, and penicillin-streptomycin were purchased from Gibco (America). Epidermal growth factor (EGF) and basic fibroblast growth factor (bFGF) were purchased from Peprotech (America). CCK-8 was purchased from Dojindo (Japan). PI and bovine serum albumin (BSA) were purchased from Sigma (Germany). TRIzol reagent was purchased from Life Technologies (America), and the *β*-actin, nestin, Tuj1, GFAP, MAP2, and Neurod1 primers for RT-qPCR were purchased from Biosune (China). DAPI and primary and secondary antibodies for nestin, Tuj1, GFAP, and MAP2 were purchased from Abcam.

Synthesis of HAp and Tb:HAp Nanorods: HAp and Tb:HAp nanorods were synthesized using the procedure described in previous work.[17] As a typical hydrothermal method, for HAp nanorods, 0.5 g 1-octadecylamine was dissolved in oleic acid (4 mL), followed by absolute ethanol (16 mL), and $Ca(NO_3)_2$ (0.28 M, 7 mL) was added while stirring. NaF (0.28 M, 1.4 mL) and Na_3PO_4 (0.168 M, 7 mL) were successively added and stirred for 10 min. Then, the mixture was transferred into a 50-mL Teflon-lined autoclave and heated at 180 °C for 12 h. Finally, the resulting products were deposited at the bottom of a 50-mL Teflon-lined autoclave. The nanorods were cleaned with ethanol and ultrapure water in a centrifuge at 10 000 rpm for 10 min, successively three times. For Tb:HAp nanorods, Tb $(NO_3)_3$ (0.28 M; 350 μL) was added to the 5 mol% Tb:HAp nanorods. For the characterization of HAp nanorods, the morphology of the HAp nanorods was assessed using SEM (Hitachi, Japan) and TEM (JEM-2100, Japan). XRD was recorded on a Bruker D8 Advance powder diffractometer equipped with a Cu K*α*-sealed tube.

Isolation, Culture, and Differentiation of mNSCs: The mNSCs were isolated from the embryos of C57/BL6 mice at embryonic day 13.5. C57/BL6 mice were purchased from laboratory animal centre (Shandong University) and the use of cells was approved by the Ethics Committee of Shandong University. Briefly, the telencephalon of the embryos was dissected out, cut into small pieces, and crushed with tweezers in phosphate-buffered saline (PBS) placed on an ice slab. The cell suspension was passed through a 70 μm cell strainer and dispersed in the cell proliferation medium.[31] For reliability, mNSCs from the third to fifth cell passage were used for the experiments.

For mNSC proliferation culture, the mNSCs were cultured in neurobasal medium supplemented with 2% B-27 supplement, 1% glutaMAX-1, 20 ng mL^{-1} EGF, 20 ng mL^{-1} bFGF, and 1% penicillin/streptomycin, and maintained in humidified air with 5% CO_2 at 37 °C. For mNSC differentiation, the mNSCs were maintained in neurobasal medium supplemented with 2% B-27 supplement, 1% glutaMAX-1, 1% FBS, and 1% penicillin/streptomycin in culture dishes pre-coated with 10 μg mL^{-1} poly(L-lysine). For the use of HAp nanorods under physiological culture conditions, a good dispersion had to be performed with an ultrasound for 15 min. The weak aggregation of HAp after repeated medium changes was to be expected and was harmless for the culture.

Live/Dead Cell Staining and Cell Viability Assay: In order to visually monitor the survival state of mNSCs, live/dead staining was performed according to the manufacturer's instructions. Briefly, the mNSCs were cultured in 48-well plates with different concentrations of HAp for 48 h,

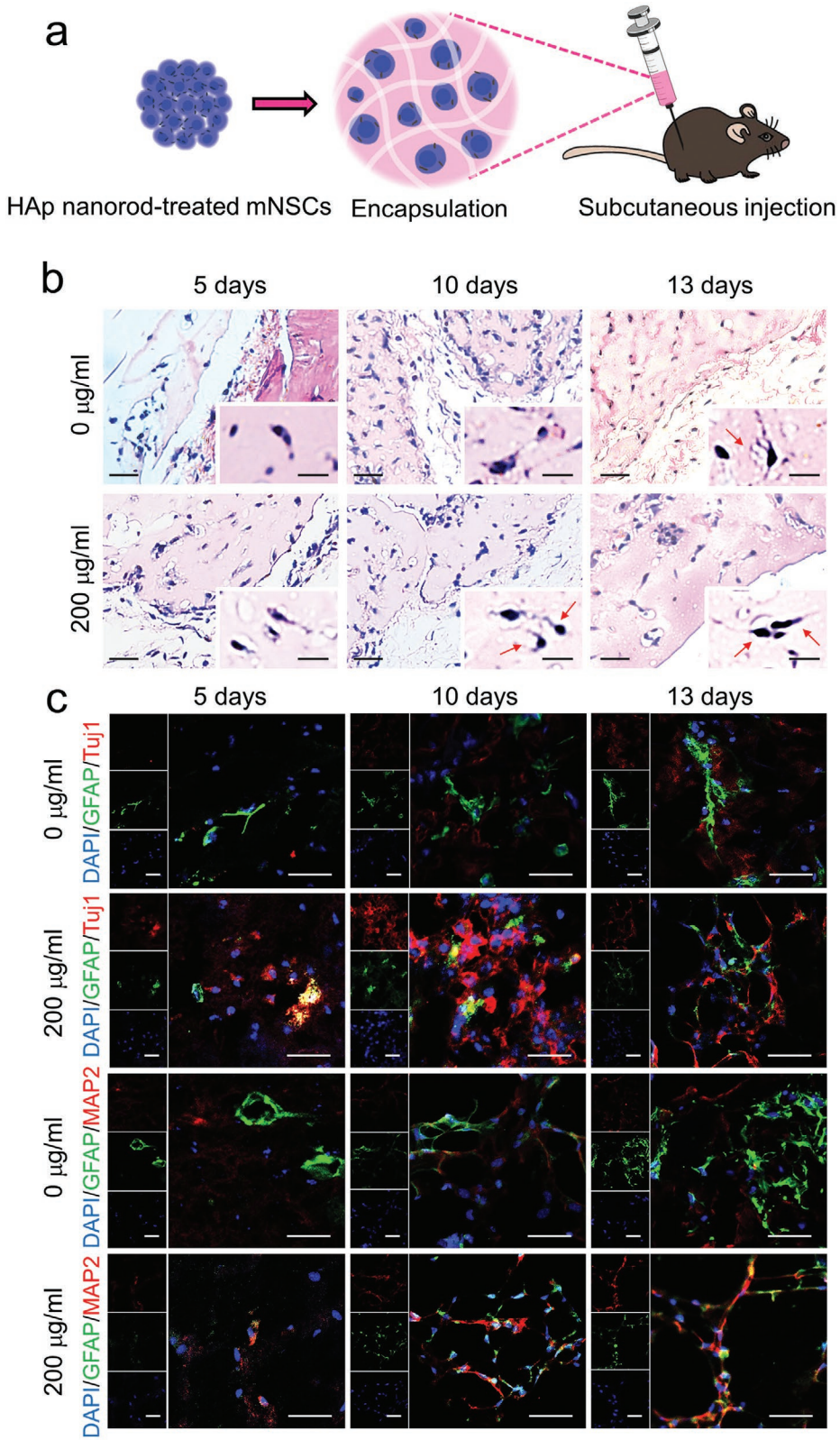

Figure 6. In vivo analysis of the survival and differentiation of mNSCs cultured with 0 and 200 μg mL^{-1} HAp nanorods. a) The procedure used for cell encapsulation and subcutaneous injection. b) H&E staining of tissue slices from animals injected with mNSCs cultured with 0 and 200 μg mL^{-1} HAp nanorods after 5, 10, and 13 days. Scale bars: 20 μm. c) Immunostaining of tissue slices for the neural-specific markers Tuj1, GFAP, and MAP2, and nuclei of the mNSCs after 5, 10, and 13 days of culture with 0 and 200 μg mL^{-1} HAp nanorods. Cell nuclei were stained with DAPI (blue), Tuj1 and MAP2 are shown in red, while GFAP is in green. Scale bars: 30 μm.

and 200 µL neurobasal medium containing 0.5×10^{-6} M calcein AM and 3×10^{-6} M PI were cultured with mNSCs. After incubation for 30 min at 37 °C, the cells were washed three times with PBS and visualized using CLSM (Zeiss Co., Germany). The ImageJ software was used to calculate the survival rate of cells after live and dead staining. Briefly, fluorescence images were imported into ImageJ, and the particles were analyzed after setting the threshold. The "Watershed" function was used to interrupt the overlapping cells, and then the automatic counting was performed. (Figure S2, Supporting Information).

For quantitative observation of cell activity, CCK-8 was used following the standard protocols described by the manufacturer. mNSCs were cultured in 96-well culture plates with cell proliferation culture medium for 1, 2, and 3 days. When the specified time point was reached, 10 µL CCK-8 solution was added to the culture medium in each well for 1 h at 37 °C, and the level of water-soluble formazan dye was assayed at a wavelength of 450 nm using a microplate reader (Multiscan MK3, Thermo, America). Triplicate parallel experiments were conducted, and the results were averaged.

TEM Analysis of mNSCs: After culturing mNSCs with or without HAp nanorods for 10 h, the cells were collected and centrifuged for 5 min at 1500 rpm. The samples were then fixed with 2.5% glutaraldehyde solution in PBS overnight at 4 °C. After washing with PBS three times, the samples were fixed with 1% osmic acid solution for 2 h. Samples were then dehydrated using gradient alcohol solutions (30%, 50%, 70%, 80%, 90%, 95%, and 100%). The sample was embedded in epoxy resin and polymerized overnight at 70 °C. Finally, the samples were sliced into ultrathin sections (70–90 nm) using an ultramicrotome (Leica EM UC7) and stained with 5% aqueous uranyl acetate and 2% aqueous lead citrate. Images were obtained using a TEM (HITACHI H-7650, Japan).

RT-qPCR Analysis: For RT-qPCR assay, the mNSCs were cultured with or without HAp nanorods for different days. On the day of RNA extraction, TRIzol reagent was used to extract total RNA, and the concentration and purity were determined using a Q-5000 spectrophotometer (Quawell, Q-5000, America) at 260/280 nm. Finally, the signals were measured using a 7500 Real-Time PCR system (Applied Biosystems, Germany) to analyze the expression of nestin, Tuj1, GFAP, MAP2, and Neurod1 (primer sequences are provided in Table S1, Supporting Information). Target gene expression was normalized to that of β-actin expression and presented as the mean ± SD.

RNA Sequencing and Analysis: RNA sequencing was performed by Shanghai Biotechnology Corporation. Briefly, mNSCs were cultured with 0 and 200 µg mL^{-1} HAp nanorods for 24 h. TRIzol reagent was used to extract total RNA following the manufacturer's instructions. Total RNA was isolated using the RNeasy mini kit (Qiagen, Germany), and paired-end libraries were synthesized using the TruSeq RNA Sample Preparation Kit (Illumina, America) according to protocols provided by the manufacturer. Briefly, the poly A-containing mRNA molecules were purified and fragmented into small pieces using divalent cations at 94 °C for 8 min. Purified libraries were quantified using a Qubit 2.0 Fluorometer (Life Technologies, America) and validated using an Agilent 2100 bioanalyzer (Agilent Technologies, America) to confirm the insert size and to calculate the mole concentration. For analysis, library construction and sequencing were performed at the Shanghai Biotechnology Corporation.

SEM Analysis of mNSC Samples: After culturing with or without HAp nanorods for 5 days, mNSCs were fixed with 2.5% glutaraldehyde solution in PBS for 30 min at 20–30 °C. The samples were then washed three times with PBS and dehydrated using an alcohol gradient (30%, 50%, 70%, 80%, 90%, 95%, 98%, and 100%). The samples were lyophilized at –60 °C for 12 h. Finally, the samples were sprayed with Au at a current of 20 µA and observed under the SEM.

Immunofluorescence Staining: After culturing mNSCs with or without HAp nanorods for 5, 10, and 13 days, the cells were washed with PBS three times and fixed with 4% paraformaldehyde at room temperature for 20 min. Then, the samples were permeabilized for 10 min with 0.1% Triton X-100 and blocked for 30 min at room temperature with 1% BSA. After blocking, the cells were incubated overnight at 4 °C with the appropriate primary antibody. A corresponding secondary antibody was applied for 1 h at room temperature. After washing three times with PBS, the cells were stained with DAPI for 5 min. Finally, the samples were observed under different excitation wavelengths using a CLSM. In order to determine the percentage of Tuj1$^+$/GFAP$^+$/MAP2$^+$ cells that were generated after mNSCs were cultured with 0 and 200 µg mL^{-1} HAp nanorods for 10 and 13 days, the number of positive cells was counted using ImageJ. At least 500 DAPI$^+$ cells were counted for the calculation. As automated cell counts by ImageJ for irregular shapes were inaccurate, manual counting was performed for DAPI$^+$, Tuj1$^+$, GFAP$^+$, and MAP2$^+$ cells. Data analysis was performed in the end (Figures S5 and S6, Supporting Information). In order to calculate the progress of the Sholl analysis, images were processed and analyzed using FIJI 2.0, ImageJ by Sholl function (Figure S8, Supporting Information).

Electrophysiological Analyses: Whole-cell patch-clamp recordings were performed at room temperature on mNSCs with HAp nanorods using an EPC-10 amplifier with Patch-Master software (HEKA, Freiburg, Germany). The recording pipette had a resistance of 3–6 MΩ when filled with an internal solution composed of 130×10^{-3} M K-gluconate, 0.1×10^{-3} M EGTA, 1×10^{-3} M $MgCl_2$, 2×10^{-3} M MgATP, 0.3×10^{-3} M NaGTP, 10×10^{-3} M HEPES, 5×10^{-3} M NaCl, 11×10^{-3} M KCl, and 5×10^{-3} M Na_2-phosphocreatine (pH 7.4). The external solution contained 110×10^{-3} M NaCl, 2.5×10^{-3} M KCl, 2×10^{-3} M $CaCl_2$, 10×10^{-3} M glucose, 1×10^{-3} M NaH_2PO_4, 25×10^{-3} M $NaHCO_3$, 0.2×10^{-3} M ascorbic acid, and 2×10^{-3} M $MgCl_2$ (pH 7.4). Signals were digitized and filtered at 10 kHz and 2 kHz. The whole-cell capacitance was compensated, and series resistance was monitored throughout the experiment to confirm the integrity of the patch seal and the stability of the recording. In this study, mNSCs with HAp nanorods cultured for 5 days were subjected to an electrophysiological study. Under the current-clamp recording, the cells were held at 0 pA, and the firing threshold was first measured by a series of 100 ms depolarizing current injections in 5 pA steps from 0 pA to elicit the first AP. In order to further examine the firing properties of neurons, a large depolarizing current (500 ms, twofold AP threshold) was delivered to elicit sufficient firing of the cell. The Origin software 8.5 (OriginLab Corporation, Northampton, MA, USA) was used for data analysis.

In Vivo Subcutaneous Injection Assay and Histological Analysis: Animal experiments followed the protocols approved by the Institutional Animal Care and Use Committee of Shandong University (20183707830197). The mNSCs (1×10^6) encapsulated in Matrigel with 0 and 200 µg mL^{-1} HAp nanorods were injected subcutaneously into 6-week-old C57/BL6 mice (200 µL volume per site, 50% Matrigel, $n = 3$ per group). After 5, 10, and 13 days, the cells formed tumors that were dissected out and subjected to H&E staining and immunostaining, according to the manufacturer's instructions.

Supporting Information

Supporting Information is available from the Wiley Online Library or from the author.

Acknowledgements

This work was supported by the National Key Research and Development Program of China (2017YFB0405400), Major Innovation Projects in Shandong Province (2018YFJH0503), the Science Fund for Distinguished Young Scholars of Shandong Province (ZR2019JQ16), the Construction Engineering Special Fund of "Taishan Scholars" of Shandong Province (No. ts20190975), the Interdisciplinary Science Innovation Group Project of Shandong University (2020QNQT001), and the Project of "20 items of University" of Jinan (2018GXRC031). The authors are thankful for the support provided by the Collaborative Innovation Center of Technology and Equipment for Biological Diagnosis and Therapy in Universities of Shandong.

Conflict of Interest

The authors declare no conflict of interest.

Data Availability Statement

Research data are not shared.

Keywords

differentiation, hydroxyapatite, neural stem cells, neurons

Received: February 2, 2021
Revised: April 20, 2021
Published online:

[1] H. Gao, J. Hong, *Trends Immunol.* **2008**, *29*, 357.
[2] O. Lindvall, Z. Kokaia, *J. Clin. Invest.* **2010**, *120*, 29.
[3] a) M. Caprnda, P. Kubatka, K. Gazdikova, I. Gasparova, V. Valentova, N. Stollarova, G. L. Rocca, N. Kobyliak, J. Dragasek, I. Mozos, R. Prosecky, D. Siniscalco, D. Büsselberg, L. Rodrigo, P. Kruzliak, *Biomed. Pharmacother.* **2017**, *91*, 60; b) N. R. Iyer, T. S. Wilems, S. E. Sakiyama-Elbert, *Biotechnol. Bioeng.* **2017**, *114*, 245.
[4] a) G. Gincberg, H. A. Zakay, P. Lazarovici, P. I. Lelkes, *Br. Med. Bull.* **2012**, *104*, 7; b) S. Suksuphew, P. Noisa, *World J. Stem Cells* **2015**, *7*, 502.
[5] P. Rebellato, Ph.D. Thesis, Karolinska Institutet, Stockholm, Sweden **2013**.
[6] A. Kimura, T. Ohmori, R. Ohkawa, S. Madoiwa, J. Mimuro, T. Murakami, E. Kobayshi, Y. Hoshino, Y. Yatomi, Y. Sakata, *Stem Cells* **2007**, *25*, 115.
[7] Y. Qian, W. E. Yuan, Y. Cheng, Y. Yang, X. Qu, C. Fan, *Nano Lett.* **2019**, *19*, 8990.
[8] D. G. Allen, H. Westerblad, *J. Physiol.* **2001**, *536*, 657.
[9] a) S. Hassanpour-Tamrin, H. Taheri, M. M. Hasani-Sadrabadi, S. H. S. Mousavi, E. Dashtimoghadam, M. Tondar, A. Adibi, A. Moshaverinia, A. S. Nezhad, K. I. Jacob, *Adv. Funct. Mater.* **2017**, *27*, 1701420; b) A. Solanki, S. T. D. Chueng, P. T. Yin, R. Kappera, M. Chhowalla, K. B. Lee, *Adv. Mater.* **2013**, *25*, 5477.
[10] R. Zhang, Y. Li, B. Hu, Z. Lu, J. Zhang, X. Zhang, *Adv. Mater.* **2016**, *28*, 6345.
[11] V. Asgari, A. Landarani-Isfahani, H. Salehi, N. Amirpour, B. Hashemibeni, S. Rezaei, H. Bahramian, *Neurochem. Res.* **2019**, *44*, 2695.
[12] a) Y. Huang, G. Zhou, L. Zheng, H. Liu, X. Niu, Y. Fan, *Nanoscale* **2012**, *4*, 2249; b) M. Hao, J. He, C. Wang, C. Wang, B. Ma, S. Zhang, J. Duan, F. Liu, Y. Zhang, L. Han, H. Liu, Y. Sang, *Small* **2019**, *15*, 1905001.
[13] C. Zhang, C. Li, S. Huang, Z. Hou, Z. Cheng, P. Yang, C. Peng, J. Lin, *Biomaterials* **2010**, *31*, 3374.
[14] a) X. Wang, J. Zhuang, Q. Peng, Y. Li, *Adv. Mater.* **2006**, *18*, 2031; b) X. Li, Q. Zou, H. Chen, W. Li, *Sci. Adv.* **2019**, *5*, eaay6484.
[15] C. M. Madl, B. L. LeSavage, R. E. Dewi, C. B. Dinh, R. S. Stowers, M. Khariton, K. J. Lampe, D. Nguyen, O. Chaudhuri, A. Enejder, S. C. Heilshorn, *Nat. Mater.* **2017**, *16*, 1233.
[16] M. Liu, T. Zang, Y. Zou, J. C. Chang, J. R. Gibson, K. M. Huber, C. L. Zhang, *Nat. Commun.* **2013**, *4*, 2183.
[17] a) M. L. Fanarraga, J. Avila, J. C. Zabala, *Eur. J. Neurosci.* **1999**, *11*, 516; b) L. Wang, L. Wang, W. Huang, H. Su, Y. Xue, Z. Su, B. Liao, H. Wang, X. Bao, D. Qin, J. He, W. Wu, K. F. So, G. Pan, D. Pei, *Nat. Methods* **2013**, *10*, 84.
[18] a) D. Laug, S. M. Glasgow, B. Deneen, *Nat. Rev. Neurosci.* **2018**, *19*, 393; b) X. Yu, J. Nagai, B. S. Khakh, *Nat. Rev. Neurosci.* **2020**, *21*, 121; c) J. A. Stogsdill, J. Ramirez, D. Liu, Y. H. Kim, K. T. Baldwin, E. Enustun, T. Ejikeme, R. R. Ji, C. Eroglu, *Nature* **2017**, *551*, 192.
[19] F. Ciaffardini, S. Nicolai, M. Caputo, G. Canu, E. Paccosi, M. Costantino, M. Frontini, A. S. Balajee, L. Proietti-De-Santis, *Cell Death Dis.* **2014**, *5*, e1268.
[20] a) T. Kuwabara, J. Hsieh, A. Muotri, G. Yeo, M. Warashina, D. C. Lie, L. Moore, K. Nakashima, M. Asashima, F. H. Gage, *Nat. Neurosci.* **2009**, *12*, 1097; b) Z. Gao, K. Ure, J. L. Ables, D. C. Lagace, K.-A. Nave, S. Goebbels, A. J. Eisch, J. Hsieh, *Nat. Neurosci.* **2009**, *12*, 1090.
[21] M. M. Pathak, J. L. Nourse, T. Tran, J. Hwe, J. Arulmoli, D. T. T. Le, E. Bernardise, L. A. Flanagan, F. Tombola, *Proc. Natl. Acad. Sci. USA* **2014**, *111*, 16148.
[22] a) S. Deng, G. Hou, Z. Xue, L. Zhang, Y. Zhou, C. Liu, Y. Liu, Z. Li, *Neurosci. Lett.* **2015**, *585*, 166; b) N. Gunhanlar, G. Shpak, M. v. d. Kroeg, L. Gouty-Colomer, S. Munshi, B. Lendemeijer, M. Ghazvini, C. Dupont, W. J. G. Hoogendijk, J. Gribnau, F. M. S. D. Vrij, S. Kushner, *Mol. Psychiatry* **2018**, *23*, 1336.
[23] a) S. T. Ahmad, A. D. Rogers, M. J. Chen, R. Dixit, L. Adnani, L. S. Frankiw, S. O. Lawn, M. D. Blough, M. Alshehri, W. Wu, M. A. Marra, S. M. Robbins, J. G. Cairncross, C. Schuurmans, J. A. Chan, *Nat. Commun.* **2019**, *10*, 2000; b) B. C. Lu, C. Cebrian, X. Chi, S. Kuure, R. Kuo, C. M. Bates, S. Arber, J. Hassell, L. MacNeil, M. Hoshi, S. Jain, N. Asai, M. Takahashi, K. M. Schmidt-Ott, J. Barasch, V. D'Agati, F. Costantini, *Nat. Genet.* **2009**, *41*, 1295.
[24] A. Gravanis, T. Calogeropoulou, V. Panoutsakopoulou, K. Thermos, C. Neophytou, I. Charalampopoulos, *Sci. Signaling* **2012**, *5*, pt8.
[25] J. Vallipuram, J. Grenville, D. A. Crawford, *Cell. Mol. Neurobiol.* **2010**, *30*, 233.
[26] Y. Y. Lu, Z. Z. Li, D. S. Jiang, L. Wang, Y. Zhang, K. Chen, X. Zhang, Y. Liu, G. C. Fan, Y. Chen, Q. Yang, Y. Zhou, X. D. Zhang, D. P. Liu, H. Li, *Nat. Commun.* **2013**, *4*, 2852.
[27] G. Abuazza, A. Becker, S. S. Williams, S. Chakravarty, H. T. Truong, F. Lin, M. Baum, *Am. J. Physiol.* **2006**, *291*, F1132.
[28] a) K. Wang, H. Wang, J. Wang, Y. Xie, J. Chen, H. Yan, Z. Liu, T. Wen, *Protein Cell* **2012**, *3*, 213; b) I. Gomes, E. N. Bobeck, E. B. Margolis, A. Gupta, S. Sierra, A. K. Fakira, W. Fujita, T. D. Müller, A. Müller, M. H. Tschöp, G. Kleinau, L. D. Fricker, L. A. Devi, *Sci. Signaling* **2016**, *9*, ra43; c) Y. Sun, L. Yao, L. Li, Y. Wang, C. Du, Y. Guo, J. Liu, *Neuropharmacology* **2018**, *137*, 275; d) C. Zhao, S. C. Gammie, *J. Histochem. Cytochem.* **2015**, *63*, 417.
[29] H. Shao, T. Li, R. Zhu, X. Xu, J. Yu, S. Chen, L. Song, S. Ramakrishna, Z. Lei, Y. Ruan, L. He, *Biomaterials* **2018**, *175*, 93.
[30] J. He, N. Zhang, Y. Zhu, R. Jin, F. Wu, *Biomaterials* **2021**, *265*, 120448.
[31] F. Sher, R. Rößler, N. Brouwer, V. Balasubramaniyan, E. Boddeke, S. Copray, *Stem Cells* **2008**, *26*, 2875.